FACTAR 2.0 CODE VALIDATION

P.B. MIDDLETON, R.C.K. ROCK, S.L. WADSWORTH

Ontario Hydro
Reactor Safety and Operational Analysis Department
700 University Avenue, Toronto, Ontario, M5G-1X6

ABSTRACT

The FACTAR code models the thermal and mechanical behaviour of a CANDU fuel channel under degraded cooling conditions. FACTAR is currently undergoing a process of validation against various data sets in order to qualify its use in nuclear safety analysis. This paper outlines the methodology being followed in this effort. The BTF-104 and BTF-105A tests, conducted at Chalk River Laboratories, have been chosen as the first in-reactor tests to be used for FACTAR validation. The BTF experiments were designed to represent CANDU fuel behaviour under typical large LOCA conditions. The two tests are summarized briefly, and the results of code comparisons to experimental data are outlined. The comparisons demonstrate that FACTAR is able to accurately predict the values of selected key parameters. As anticipated in the validation plan, further work is required to fully quantify simulation biases for all parameters of interest.

1. INTRODUCTION

The fuel channel thermal mechanical code, FACTAR 2.0 [1], is being validated using a standardized validation methodology. This process has been recently adopted by the Canadian nuclear industry [2]. The first application of this process to FACTAR addresses predictions of key channel integrity parameters associated with large Loss of Coolant (LOCA) licensing scenarios. These parameters include UO_2 temperatures, fuel sheath temperatures, and pressure tube average strain for combinations of cooling flows and power transients which produce conditions prototypic of a large LOCA. Parameter values are governed by the interaction of various physical, chemical and thermodynamic phenomena which could potentially occur in a given accident scenario. For large LOCA, a specific validation plan has been developed to identify biases, and thereby assess the accuracy of the code calculations of these parameters. The Fuel and Fuel Channel Validation Matrix document is used as a resource to identify data sets in which the primary phenomena are represented. Implementation of this plan will lead to an assessment of whether the primary phenomena and their interactions are realistically represented by the FACTAR modeling.

2. DESCRIPTION OF TESTS USED

Currently, validation work includes individual model validation in parallel with integrated code validation. The first two data sets chosen for integrated code validation are the BTF-104 [3] and BTF-105A [4] experiments conducted in the Blowdown Test Facility (BTF), installed in the NRU reactor at Chalk River Laboratories [5]. Each of these tests subjected a single CANDU fuel element, operating in a steam cooled environment in a vertical test section, to a blowdown depressurization. In both tests, the blowdown phase was followed by a stepped power transient under conditions of degraded steam cooling. BTF-104 and BTF-105A provided validation data for conditions prototypic of the early and late blowdown periods of a large LOCA.

The BTF-104 test took place in September 1993, and BTF-105A took place in March 1996. In both experiments, the test section, encompassing the fuel element, coolant flow annuli, and surrounding thermal insulation, was instrumented with thermocouples to record the transient thermal response of these components. In addition, pressure transducers and flow meters were installed to measure coolant conditions. During the BTF-104 test, difficulties were encountered with fuel sheath instrumentation, and only qualitative trends were obtained. Post Irradiation Examination (PIE), however, yielded information on the distribution and extent of fuel sheath oxidation. The experiment proved useful to demonstrate that the integrated sub-models within the FACTAR code interact to produce realistic predictions. Figure 1(A) provides an illustration of the BTF-104 test section, and indicates the approximate location of thermocouple instrumentation which is referred to in this paper.

The BTF-105A experiment featured improved instrumentation technology, and fuel centreline thermocouples. As a result, fuel element temperatures were successfully recorded. BTF-105A provided superior transient data, however, coolant flow rate boundary conditions were more variable than in BTF-104. For reference, a schematic diagram of the BTF-105A test section is provided in Figure 2(A).

3. DESCRIPTION OF CODE VERSION AND DATA SETS USED

The FACTAR code series was developed in order to model the thermal and mechanical response of a CANDU fuel channel under LOCA conditions. As a result, a typical application involves the representation of a string of fuel bundles, in a coolant channel bounded by a pressure tube/calandria tube assembly. Since data from full scale components under accident conditions are not available for a nuclear heating environment, the code must be validated against smaller scale experiments. As a result, the code model must be adaptable to the available experimental apparatuses.

The central task in the validation exercise involves representing the experimental apparatus and the test conditions using code input data. The input data required to do this can be classified according to the following categories:

- geometry;
- materials and their physical properties;
- initial (steady-state) conditions; and
- transient conditions.

FACTAR 2.0 contains a generalized geometry specification which can be used to represent the BTF test-section. The code contains thermodynamic properties for both H_2O and D_2O coolant. As a result, the base version of the FACTAR 2.0 code was appropriate for performing validation exercises using data obtained from BTF tests. The resulting idealization, as represented by FACTAR 2.0, is summarized as:

- a multi-segment or single segment fuel element, concentric within a single flow channel, which employs the same axial segmentation as the fuel;
- the thermal shroud, represented as a specified number of solid layers, bounded by gap resistances (the shroud retains a fixed geometry throughout the simulation);
- axisymmetric conditions; and
- a representation of a CANDU-prototypic fuel element. Endcaps, and appendages are not modeled. A central hole used to house the centreline thermocouples was included in BTF-105A simulations.

To characterize the test section, details of geometry, fuel element soak irradiation history, materials used, and their thermophysical properties, were required. These were obtained from and verified by the experimental group. The initial and transient conditions were obtained either directly or indirectly from measurements recorded before, during and after the transient phase of the experiment. Care was taken that proper quality assurance practices were employed in the development of this data set.

The best approach to assuring data set quality is to use directly measured experimental data wherever possible. This experimental data is initially qualified by separating the measured parameters into three groups: (a) qualified data; (b) trend data; and (c) failed data. Only qualified data is used in the data sets with trend data used under certain circumstances when it can be collaborated from other sources.

Qualified data sets have been prepared for the FACTAR validation exercises using data from tests BTF-104, and BTF-105A. Conditions in the BTF test section during these tests are illustrated in Figure 3 and Figure 4, respectively.

4. COMPARATIVE ANALYSIS OF CALCULATION AND EXPERIMENT

4.1 BTF-104 Comparisons

This section describes comparisons between a FACTAR simulation, referred to as the 'nominal case', and results from the BTF-104 test. The nominal case was conducted using the best-estimate experimental conditions (Figure 3) , consisting of fuel power, test section coolant pressure, coolant flow rate, and coolant enthalpy at the elevation of the top of the element[1]. The radial boundary condition was obtained using the average of the transients recorded by the 'TSTO' thermal shroud thermocouples[2]. This representation is illustrated in Figure 1(B). The only transient data available for comparison came from the interior shroud 'TSTI' thermocouples. PIE, however, included measurement of the thickness of zirconium oxide which formed on the sheath surfaces over the course of the transient.

4.1.1 Sheath Oxide Thickness

The oxide thickness measured on the sheath outer surface are plotted in Figure 5(A). The plot indicates that the slope of the oxide thickness increases as a function of distance from the top of the fuel stack. Both the data and the code calculations for the nominal case can be successfully fit to an exponential curve as a function of distance along the element. Such a curve ignores the effect of appendages such as bearing pads, which are expected to act as cooling fins, producing a localized sheath temperature reduction. The curve can be used to clearly illustrate such deviations from the overall trend within the data. The code itself does not account for this geometric complexity, and thus, predicts that the oxide thickness increases monotonically with distance along the element. The measured data points at 42 mm, 251 mm and 269 mm indicate values which are somewhat lower than the exhibited trend. The location of the bearing pads is indicated by heavy lines on the x axis of Figure 5(A). These show that the points at 42 mm. 251 mm, and 269 mm, may indicate such regions of cooler temperatures. The point at 387 mm is a bearing pad length upstream of the nearest appendage, and its low oxide thickness is not likely indicative of this effect[3].

In the nominal case, the code predicted outer surface oxide production which ranged from an overprediction of 13% at the top of the element, to an underprediction by 13% at the bottom of the element[4]. Because the coolant flow rate was relatively constant, the sheath

---

[1] Enthalpy was calculated for superheated steam using measured temperature and pressure, using light water steam tables.

[2] There was little temperature variation along the length of the outside of the thermal shroud, due to its insulating properties, and the effect of the bypass coolant flow.

[3] The deviation may be attributed to asymmetric temperatures, or uncertainty in the original location of the measured sheath fragment.

[4] These values are with respect to the curve fit through the mean oxide thickness data points

temperature evolution was governed primarily by the power transient. As a result, the sheath oxide thickness provides a good indication of the sheath temperature history. The deviation in measured and predicted oxide thickness suggests overprediction of the temperatures at the top of the element, and underprediction at the bottom. This assertion is supported by the metallurgical evidence which suggests maximum sheath temperatures of approximately 900°C at the top of the element, and minimum temperatures of approximately 1500° C over the bottom 116 mm. The temperatures at the top of the element may have been biased downward by a small amount due to heat transfer by conduction to the convectively cooled hangar bar. The temperatures at the bottom of the element did not likely exceed 1500°C by a significant margin. This conclusion is suggested by the presence of sheath material in this region which was not completely oxidized. At temperatures in excess of 1500°C, rapid through-wall oxidation would have been expected.

The FACTAR oxidation model was used to estimate an end-of-transient sheath temperature which would result in a predicted oxide thickness equal to each available PIE measurement, including upper and lower bounds. This resulted in an axial profile of the expected sheath temperature just before the reactor shutdown was initiated. These temperatures are provided in Figure 5(B), and strengthen the conclusion that FACTAR has captured the magnitude of the sheath temperatures during the test, but has not succeeded in defining the axial profile accurately.

4.1.2 Thermal Shroud Interior Temperatures

The code calculations of thermal shroud interior temperatures are plotted against thermocouple data in Figure 5(C). The FACTAR data used to compare with these measurements is a calculated gap temperature which is assumed equal to the mean of the bounding Nilcra and Zircaloy temperatures. The thermocouples that were used to obtain the data were located in vertical rectangular channels manufactured into the outside surface of the Nilcra portion of the thermal shroud. The channels were bounded on the outside by the innermost Zircaloy shell. As a result, they indicate a Nilcra outer surface temperature that is biased by the thermocouple's exposure to the fluid environment in the channel. It is known that at some point in the test, steam was able to enter this space, either by flowing downward between the Nilcra and the Zircaloy, possibly using the thermocouple channel as a conduit, or by ingression through cracks in the Nilcra[5]. Cracks were observed during the PIE that lead directly to the thermocouple wells, probably due to their effect as a stress concentrator.

The code assumes that the thermal shroud geometry remained fixed during the course of the test, and hence that the gap thickness was equal to the manufactured radial clearance

---

[5] At times where the inlet coolant was saturated, the interior shroud thermocouples indicated the saturation temperature, a strong indication of the presence of coolant at the measurement locations.

between the shroud components. The axisymmetric heat transfer model does not account for the presence of the thermocouple wells, or the possibility of radial cracks. Since the code can only model a stagnant fluid condition, the possibility of steam flow through the gap and / or thermocouple well is not simulated.

Figure 5(C) reveals that the code's predictions of the shroud temperature response exhibits more gradual slope changes in response to the power steps than do the actual thermocouple data. The data at 3250 s, 3400 s, 3600 s, and 3900s show distinct slope changes, while the code predictions indicate more smoothly varying trends.

The code predicted temperatures at the mid and bottom planes do not reach the values exhibited by the thermocouples in the period just prior to shutdown, where thermocouple TSTL06 rapidly passed through 1250 °C, tripping the reactor and terminating the test. The sudden drop in measured temperature recorded by TSTLO2 and TSTL06 at 4250 s, was postulated to have occurred as a result of coolant condensing on the inside of the pressure tube, and occasionally being flushed through the test section. The presence of coolant flow on the exterior of the Nilcra may have dropped the indicated temperatures rapidly, before allowing them to recover to the level of the nearby shroud solid surfaces. This effect would explain the apparent discrepancy in the time response between the code predictions and experimental measurements. The underprediction of peak shroud temperatures is consistent with the evidence that sheath temperatures at the bottom of the element were underpredicted.

4.2 BTF-105A Comparisons

This section describes comparisons between a FACTAR simulation and results from the BTF-105A test. As in the BTF-104 case, the FACTAR simulation was conducted using the best-estimate experimental boundary conditions (Figure 4). The radial boundary condition was obtained using the transients recorded by the 'TSTI' interior thermal shroud thermocouples. This representation is illustrated in Figure 2(B). There was a significant axial variation in the temperature recorded by these devices, and for this reason, the temperatures input to the code were specified at each axial segment using values interpolated/extrapolated from measurements. The use of the interior shroud as a boundary condition also helped to reduce the simulation bias introduced by coolant flow into the Nilcra / Zircaloy gap.

For the BTF-105A test, transient data was available to compare to code predictions of coolant, sheath, and fuel centreline temperatures. At the time this paper was written, oxide data was not available from PIE.

4.2.1 Coolant Temperature

The FACTAR calculated coolant temperatures are plotted for comparison to the temperatures measured by thermocouples TC08B and TC09B in Figure 6(A). The measured coolant temperatures were taken at a location 4 cm below the bottom of the fuel stack (FACTAR calculates coolant temperature only to the bottom of the fuel), and thus are somewhat displaced with respect to the calculated values they are being compared to.

The hot junctions of the coolant thermocouples, while protruding into the central flow annulus over the fuel, were located beneath a centering spider, and thus had some shielding from radiative heat transfer from the bottom of the fuel element, when it reached elevated temperatures. Radiated energy, if absorbed by the thermocouple, would tend to bias the measurement upwards. These devices exceeded their operational limit at about 2900 s into the transient when peak sheath temperatures likely reached 1700°C[6]. Without shielding from the centering spider, radiative biasing of the thermocouples would be an issue at this temperature.

Until 2400 s in the transient, coolant temperatures agree most closely with measurements made with device TC08B. The general agreement with the average of TC08B and TC09B is quite good for the first 1700 seconds of the experiment. The upward and downward spikes which are observable at about 100 s intervals, most prominently between 1600 and 2100 s, are an artifact of the technique used to evaluate the coolant flow rate in the absence of direct flow measurements in the test section. As described in Reference 4, the flow transient was developed using the slope of the blowdown tank mass transient, corrected for pressure variations between the interior and exterior of the tank, and compressibility effects of trapped gas. The choice of the differentiation intervals was somewhat arbitrary, and the noisiness of the original signal was carried through with the differentiation process. Note however, that the time-averaged agreement between code and experiment is quite good[7] in the interval between 0 and 2900 s. The degree of smoothness of the measured data gives an indication that such low frequency variation was not present in the actual flow rate.

Centered on 2000 s is a sudden prolonged drop in predicted outlet coolant temperature, which, again is thought to be an artifact of the differentiation process used to produce the flow rate transient. This is evidenced by the fact that the predictions of fuel sheath and centreline temperatures also undergo large deviations below the measured trends over this period. A study using measured coolant temperatures as boundary conditions indicates that these deviations are almost entirely due to this noise.

At the local peak in measured temperatures observed at 2400 s, the code prediction most closely tracks the measurement from device TC08B. The two thermocouple tips were located on opposite sides of the flow channel. Asymmetric cooling conditions, or other

---

[6] An approximate value, inferred from strapped thermocouple measurements, and code calculations.
[7] The time-averaged difference between the FACTAR prediction, and the mean of TC08B and TC09B was 2°C, while the RMS difference was 60°C (the noise dominates the RMS error).

environmental factors (not modeled by FACTAR) could have produced a true physical difference in the coolant temperature that these two thermocouples were exposed to. From 2500 s until the time at which the instrument signal reached full-scale, the code trend was to underpredict the measurement by about 100°C. The code is likely also underpredicting sheath temperatures as well, if one accounts for biasing of TFS04 (as explained in section 4.2.2). The fact that coolant temperatures appear underpredicted at this point has implications on fuel element predictions because coolant temperature is a boundary condition for the fuel thermal model. At 3000 s, the predicted temperature corresponded to the maximum enthalpy for which steam properties are available in the code, and thus predictions are not usable after this point.

4.2.2 Sheath Temperatures

Three of the BTF-105A fuel sheath thermocouples are judged to have provided reliable data for the bulk of the transient period, these being TFS02, TFS03 and TFS04 [4]. The data provided by the clamped thermocouples, TFS02 and TFS03, is difficult to interpret, because the presence of the clamp strap has a biasing effect on the measurement with respect to the true temperature of the underlying sheath. In fact, code studies show that in the local vicinity of the thermocouple, the strap can perturb the fuel and sheath temperatures from the trend which would have occurred in the absence of the strap. This is true also of the thermocouples attached by welding, of which TFS04 is an example, though the effect is believed to be much smaller. In general, smaller diameter devices provide less of a biasing effect, but present survivability problems in an in-reactor test.

As a consequence, it was decided to compare the FACTAR predictions only to the functioning welded thermocouple, TFS04 (Figure 6(B)). The results of the comparison provide support to the intuitive suspicion that the bias would be largest during periods of relatively high flow rate, where the fin efficiency of the device would increase. The first such instance where the thermocouple bias is apparent is during the initial high power period which extended into the first 125 seconds of the transient time. During this relatively steady, high flow period, the predicted temperatures exceed the indicated temperature by about 75° C. If TFS04 were providing a true indication of the sheath temperature, such a discrepancy would imply a factor of three error in the effective convective heat transfer coefficient from the sheath to the coolant. A significant finning bias is probably in effect again during the period from 2400 s to 2600s when coolant flow rate increased, driving the test section temperatures downward. In general, though, the magnitude of the predicted temperatures is within 100°C of the indicated values over the whole of the transient. As mentioned in section 4.2.1, the noise in the coolant flow rate transient contributes to the deviation of the measured and predicted trends at some points, particularly in the period between 1800 and 2300 s. Sensitivity cases using measured coolant temperatures as a boundary condition demonstrate that during low flow periods, the deviations between experimentally measured TFS04 and the code are almost entirely attributable to the error in power to coolant. The fact that the mean magnitude is close to

the measured values may attest to the accuracy of the total integrated flow, and the chosen flow split[8].

4.2.3 Centreline Temperature

A comparison of FACTAR predictions to the measured TFC02 temperatures is provided in Figure 6(C). As discussed in section 4.2.2, thermocouple straps appear to perturb the underlying fuel temperatures. Since FACTAR does not model this effect, and since TFC01 was located in one of these regions, it was decided to compare the code predictions only to TFC02. It is not expected that the thermocouple straps would appreciably affect the temperatures at other locations far removed from the straps. Because the width of the straps is very small in relation to the length of the element, and because the transport time of the coolant over the element is quite short, the straps will not greatly affect the axial profile in coolant temperature. In other words, the effect of the coolant velocity and conduction along the element is to axially smooth the effect of the straps. Similarly, the temperature profile on the interior of the thermal shroud will not be appreciably impacted. The sheath communicates directly with the thermal shroud via thermal radiation. The presence of the strap provides an impedance in the radiation path between the sheath surface beneath the strap and the shroud, as energy is intercepted by the strap. The beneath-strap sheath surface can still 'see' the shroud, however, though less effectively than would occur without straps. As a result, the measurements taken at the locations of TFS04 and TFC02 can be compared directly with simulations which do not address the effect of the straps.

Initially, the centreline temperatures are not well predicted, being about 100 °C too low. The reason for the discrepancy is not evident. One possible explanation is that the element power was underestimated. If this were true, then the coolant temperature predictions would likely be too low, unless the flow rate was coincidentally underestimated. In turn, the convective coefficients would have to be biased low as a function of flow rate to explain the degree of agreement in the transient sheath and fuel centreline temperatures. As a result, the apparent level of agreement between code and experiment would have to be a result of fortuitous cancellation of errors if the fuel power were truly underestimated.

For the period between 125 seconds and the time of element failure, the agreement between TFC02 and the FACTAR predicted value is generally within 100°C, with the RMS difference amounting to 84°C. The deviation below the measured trend in the period between 1900 and 2250 s is attributable to the deviation in coolant temperature, since the coolant temperature represents a boundary condition to the fuel element model. The sensitivity study using measured coolant temperatures as a boundary condition demonstrated that fuel element temperatures are generally underpredicted, however.

---

[8] The test section flow consisted of the central flow path over the fuel element, and the bypass flow over the exterior of the thermal shroud. During the transient 80% of the flow was assumed to pass over the fuel.

5. CONCLUSIONS AND RECOMMENDATIONS

- The data from the BTF-105A simulations indicate that the code is capable of predicting transient fuel and sheath temperatures to within ± 100° C for a low burnup fuel element subjected to degraded steam cooling and sheath temperatures approaching the threshold of high-rate sheath oxidation (*i.e.* peak sheath temperatures in the vicinity of 1500° C). BTF-104 simulations produced comparable accuracy in sheath temperature predictions for a moderate burnup element.
- The code-predicted sheath oxide profile intersects the curve-fit through the measured sheath oxide thickness for the BTF-104 test, but does not match the axial distribution.
- The only transient indications of the BTF-104 test section response came from the Nilcra liner thermocouples. The code does not account for the possibility of coolant flow through the thermocouple channels, and this bias impeded interpretation of the results.
- As anticipated in the validation plan, further integrated code validation, against additional data sets, is recommended to more rigorously quantify the accuracy of FACTAR predictions.
- Since the BTF tests were designed to acquire information of fuel thermal behaviour, additional specialized tests are required to assess the accuracy of the fuel mechanical response models.

6. ACKNOWLEDGMENTS

The authors wish to acknowledge the close cooperation of the BTF team at Chalk River Laboratories, who provided indispensable help in assuring the accuracy of the FACTAR representation of the BTF tests. The experimental data was made available through the cooperation of the CANDU owners group, consisting of the Canadian nuclear utilities, and AECL.

7. REFERENCES

(1) Westbye C.J., Mackinnon J.C., Gu B.W., Ballyk J.D., Brito A.C., Evens D., Rock R.C.K., *The Fuel and Channel Thermal/Mechanical Behaviour Code FACTAR 2.0 (LOCA)*, Presented at the 17th Annual Canadian Nuclear Society Conference, Fredericton, New Brunswick, Canada, June 9-12, (1996).

(2) Middleton P.B., Wadsworth S.L., Rock R.C.K., Sills H.E., Langman V.J., "FACTAR Validation", presented at the Fourth International Conference on CANDU Fuel, Pembroke, Ontario, Canada, October 1-4, (1995).

(3) Dickson, L.W., DeVaal, J.W., Irish, J.D., Elder, P.H., Jonckheere, M.G., and Yamazaki, A.R., "The BTF-104 Experiment: An In-Reactor Test of Fuel Behaviour, and Fission-Product Release and Transport Under LOCA/LOECC Conditions", presented at the Fourth International Conference on CANDU Fuel, Pembroke, Ontario, Canada, October 1-4, (1995).

(4) DeVaal, J.W., Irish, J.D., Dickson, L.W., Craig S.T., Jonckheere, M.G., and Bourque L.R., "Preliminary Results of the BTF-105A Test: An In-Reactor Instrument Development and Fuel Behaviour Test", to be presented at the Fifth International Conference on CANDU Fuel, Toronto, Ontario, Canada, September 21-25, (1997).

(5) Walsworth J.A. et al., *The NRU Blowdown Test Facility Commissioning Program*, Presented at the Tenth Annual Canadian Nuclear Society Conference, Ottawa, Ontario, June 6 to 7, (1989).

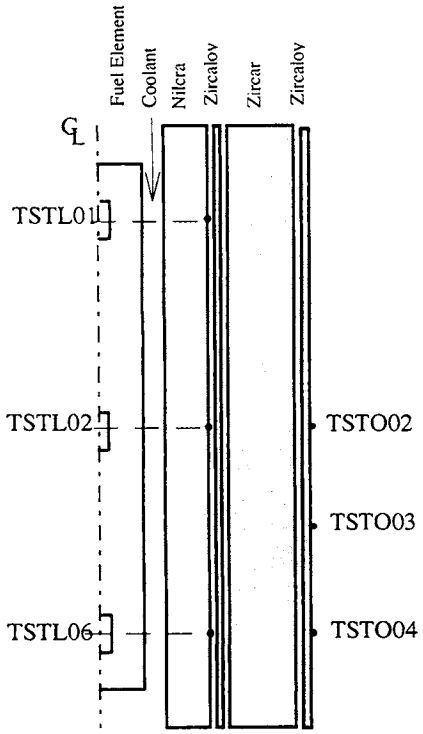

FIGURE 1(A)
SCHEMATIC DIAGRAM OF BTF-104 TEST SECTION, ILLUSTRATING SELECTED INSTRUMENTS

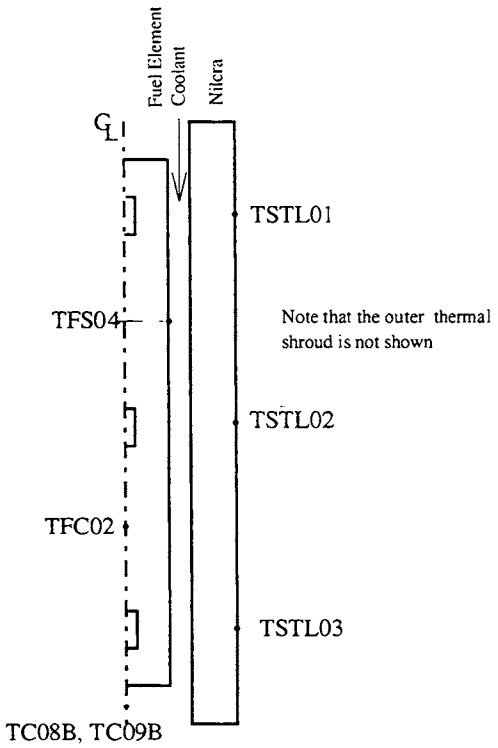

FIGURE 2(A)
SCHEMATIC DIAGRAM OF BTF-105A TEST SECTION, ILLUSTRATING SELECTED INSTRUMENTS

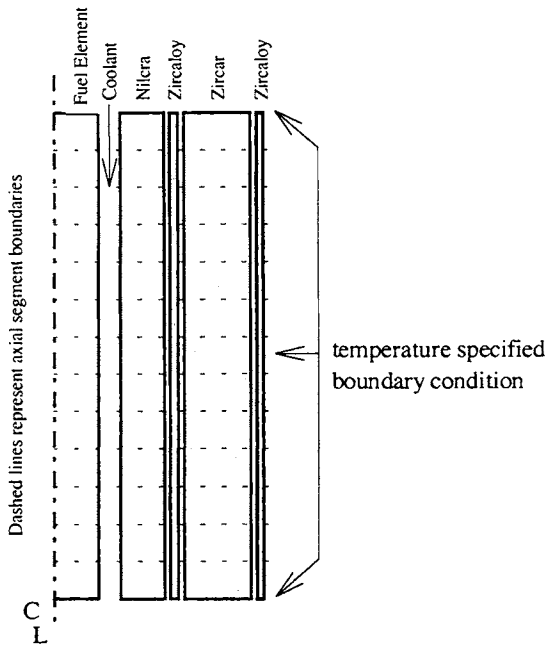

FIGURE 1(B)
SCHEMATIC DIAGRAM OF FACTAR REPRESENTATION OF BTF-104 TEST SECTION

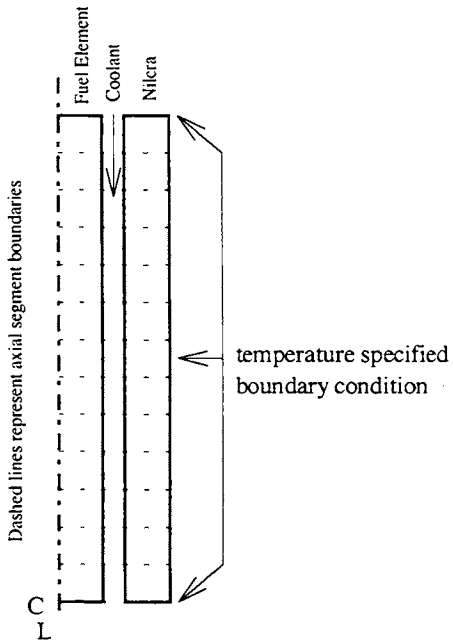

FIGURE 2(B)
SCHEMATIC DIAGRAM OF FACTAR REPRESENTATION OF BTF-105A TEST SECTION

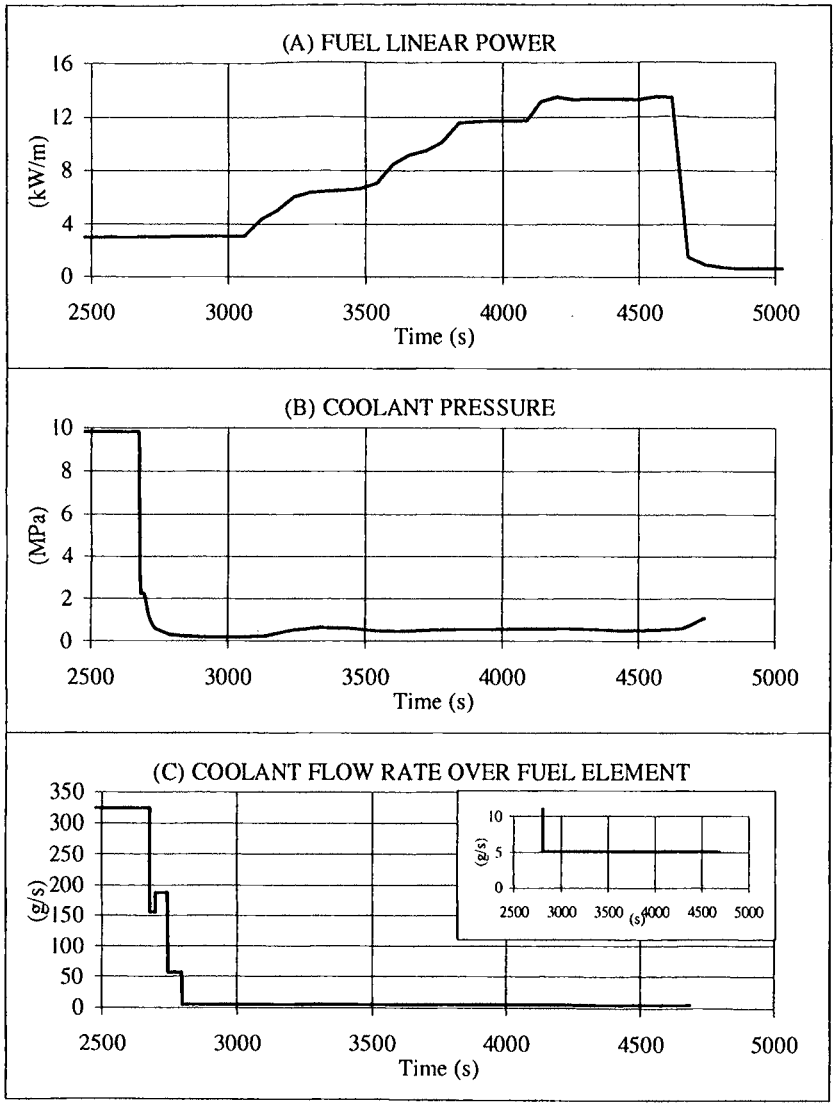

FIGURE 3
CONDITIONS DURING BTF-104 BLOWDOWN PHASE

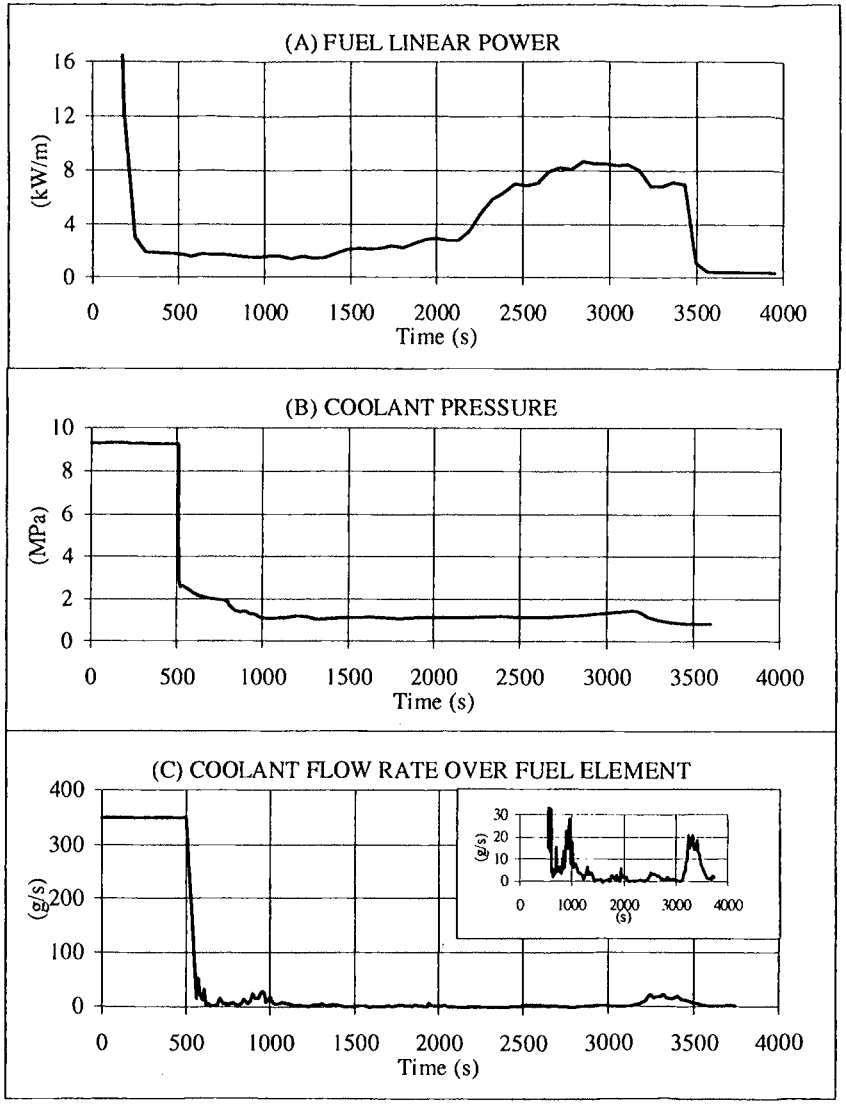

FIGURE 4
CONDITIONS DURING BTF-105A BLOWDOWN PHASE

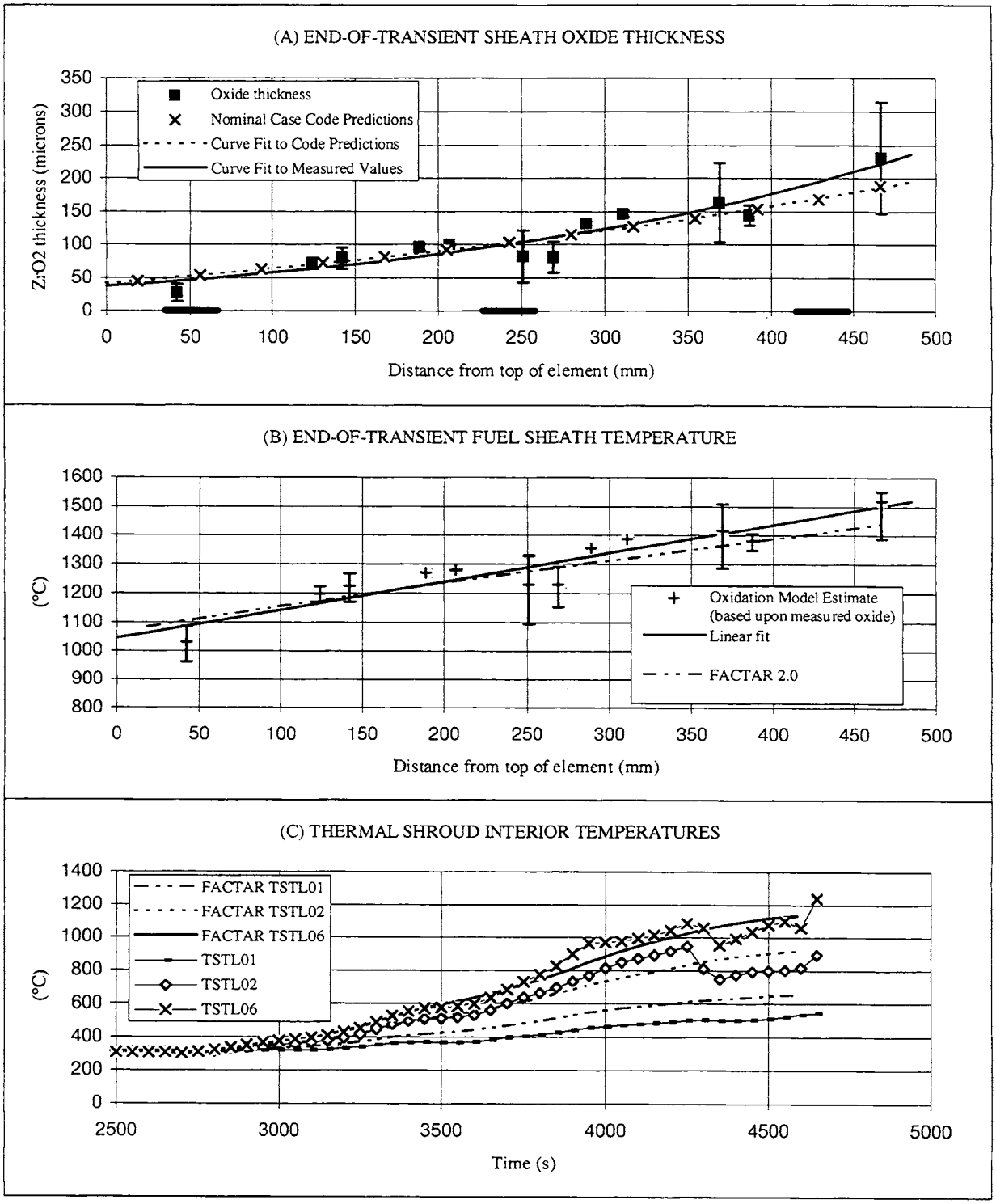

FIGURE 5
COMPARISON OF BTF-104 DATA WITH FACTAR 2.0 PREDICTIONS

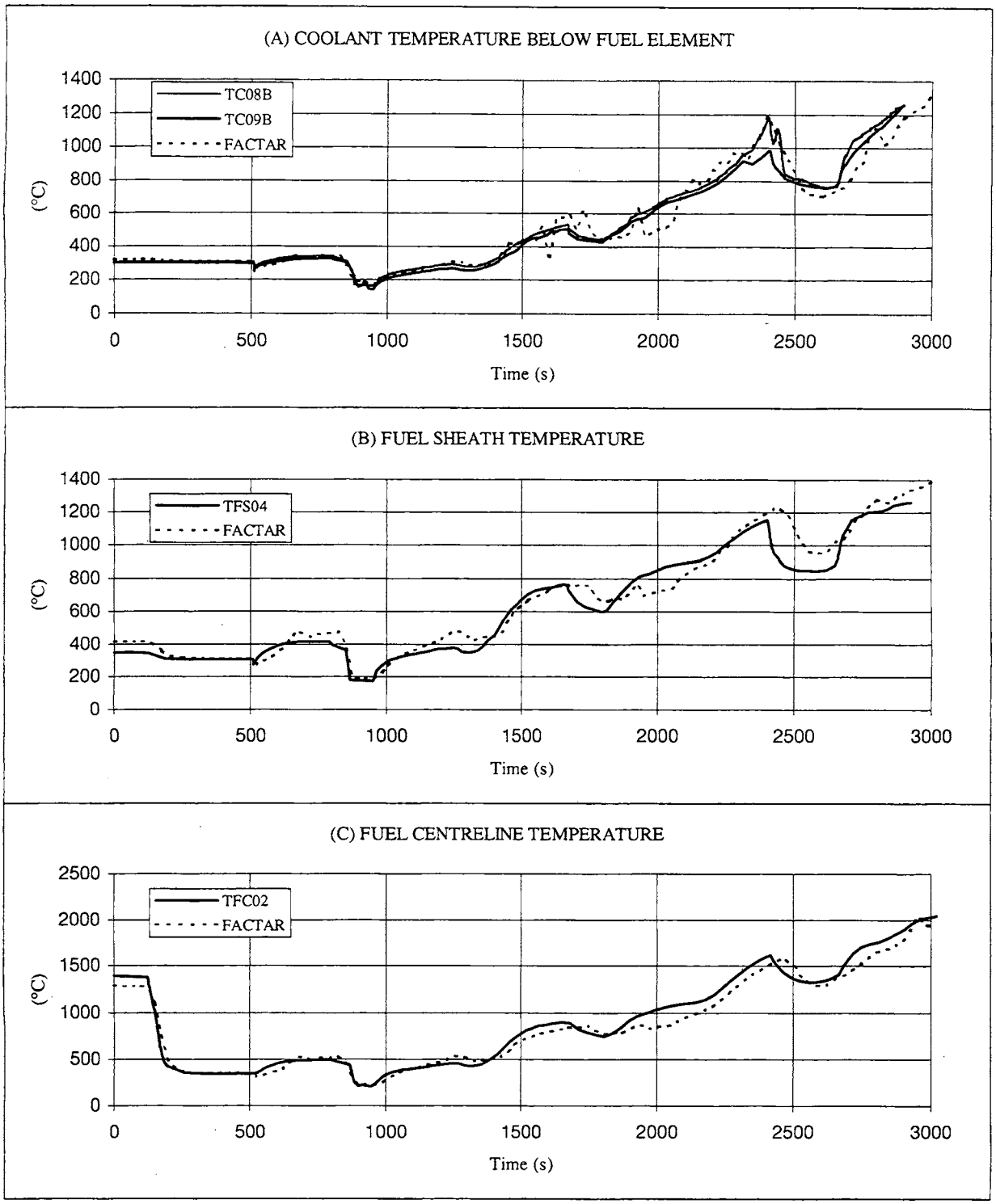

FIGURE 6
COMPARISON OF BTF-105A DATA WITH FACTAR 2.0 PREDICTIONS